Performance of geogrids overlying geotextiles in roadway stabilization applications

Christopher, B. R.
Christopher Consultants, Roswell, Georgia USA

Schwarz, L.G.
Geocomp Corp / GeoTesting Express Inc., Alpharetta, Georgia USA

Keywords: Geogrid, geotextile, geocomposite, stabilization, reinforcement, separation, subgrade, base, roadway

ABSTRACT: Geosynthetic reinforcement used in pavement systems typically can be delineated by their capabilities to provide improvement by employing and enhancing the mechanisms of separation/filtration and interlock. Geogrids and geotextiles can be used in a layered reinforcement system to provide the advantages of both materials. Alternatively, geocomposites combine both a geogrid and geotextile into a single layer material. Notwithstanding previous research demonstrating the benefits of geogrid reinforcement, little is known regarding the performance of combinations that include layering geogrids over geotextiles. Presented in this paper are the results of full-scale laboratory stabilization testing on several different geogrid/geotextile systems in unpaved roadway sections. The pavement test box facility is designed to mimic pavement layer materials, geometry and loading conditions encountered in the field while allowing a high degree of QC/QA to be exercised on the construction and control of subgrade/aggregate material properties. A brief description of the test section construction procedures, equipment, materials, instrumentation and test protocol is presented. The results of the full scale tests in terms of rutting in the four geosynthetic test sections and the control section, and the pore pressure measurements and stress strain response of the geogrid in each full scale test are used in the comparison of each test section's performance. A post construction evaluation of the geogrid/subgrade and geogrid/geotextile interface is provided. A clear difference was observed in the performance of the geosynthetic systems evaluated in this study.

1 INTRODUCTION

Geogrid reinforcement of the aggregate layers in construction platforms, temporary roads and pavement systems increases load carrying capacity, reduces excessive deformation of the roadway surface, and enhances the stiffness of the material adjacent to the geosynthetic reinforcement. The predominant reinforcing mechanism associated with this application is base course lateral restraint. However, the performance of geogrids can be compromised if fine grain subgrade soil migrates into the aggregate layers. It only takes a small amount of fines to significantly affect the structural characteristics of select granular aggregate (e.g., Jornby and Hicks, 1986) and thus jeopardize the performance of geogrid reinforcement. Therefore, a geotextile separator is often used beneath a geogrid to prevent migration of fines into the aggregate layers over time. Notwithstanding previous research demonstrating the benefits of geogrid reinforcement,

little is known regarding the performance of combinations that include layering geogrids over geotextiles, either by simply placing the geogrid over the geotextile or as a geocomposite.

Combining a geogrid with a geotextile does create some concern that interlock will be diminished thus reducing the effectiveness of the geogrid. Also, the interface friction between a geogrid and geotextile is relatively low compared to the interface friction of either material with the soil, which could also result in reduced performance due to slippage between the geogrid and geotextile. In order to evaluate these perceived concerns, a series of full scale laboratory stabilization tests were performed on several different geogrid/geotextile systems in unpaved roadway sections. The same type of geogrid reinforcement was evaluated in four separate test sections consisting of (a) the geogrid only, (b) the geogrid placed over a needlepunched nonwoven geotextile, (c) the geogrid overlying a heat-bonded nonwoven geotextile, and (d) a manufactured

geocomposite consisting of the geogrid bonded to a needlepunched nonwoven geotextile. Control tests without geosynthetics were also performed. A brief description of the stabilization test program follows. Comparison of the results of the full scale laboratory stabilization tests performed on each of these different geogrid/geotextile systems in unpaved roadway sections is provided.

2 STABILIZATION TESTING PROGRAM

The GeoTesting Express pavement test box shown schematically in Figure 1 was used to create the test sections presented herein. The pavement test box facility was designed and constructed for the purpose of conducting full-scale laboratory experiments on reinforced and unreinforced pavement sections and it meets the requirements of specifications developed for AASHTO Subcommittee 4E as contained in Berg et al. (2000). The test box facility is designed to mimic pavement layer materials, geometry and loading conditions encountered in the field as realistically as possible with an indoor, laboratory based facility (Perkins, 1999, 2002). This type of test box facility allows a high degree of control to be exercised on the construction and control of pavement layer material properties.
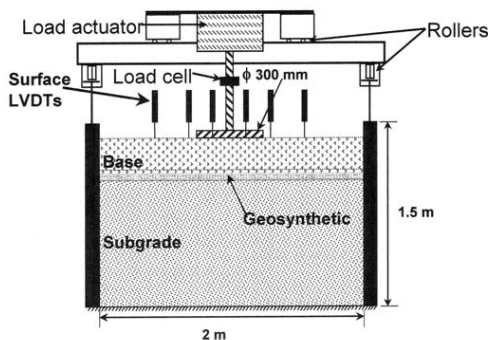

Figure 1. Schematic diagram of the pavement test facility.

Each roadway test section was constructed with a nominal cross-section consisting of 300 mm of base course aggregate and 1.1 m of subgrade soil with a CBR=1. The cyclic load tests followed the procedures in the American Association of State and Highway Transportation Officials (AASHTO) PP 46-01. Each test section was constructed in a test box with dimensions of 2 m length, 2 m width, and 1.5 m height shown utilizing residual silt (ML-MH) subgrade and a graded aggregate base that met the Georgia Department of Transportation

specifications. Each test section was instrumented to evaluate (a) rutting in the stabilization aggregate, (b) strain distribution in the reinforcement with distance away from the applied load, and (c) pore water pressure response of the subgrade. As indicated in the Introduction section, the geosynthetics were placed between the base course and subgrade layers in four tests. Control tests without geosynthetics were also performed.

A cyclic, non-moving load with a peak load value of 40 kN was used to mimic dynamic wheel loads. Sensors were used to measure applied pavement load, pavement surface deformation, and stress and strain in the base aggregate and subgrade soils.

Instrumentation was used in each test section to evaluate rutting in the stabilization aggregate, strain distribution in the reinforcement with distance away from the wheel load, and pore water pressure response of the subgrade during placement, compaction, and subsequent loading.

The complete details of the box setup and description of the instrumentation used in this program are reported by Christopher and Lacina (2008) and Christopher, B.R. and Perkins, S. W. (2008) for similar stabilization studies.

2.1 Geosynthetic Materials

Four geosynthetics were used in this study: [1] a welded polypropylene biaxial geogrid (GG_{wd-pp}), [2] a 151 g/m^2 polypropylene needlepunched nonwoven geotextile (GT_{np-nw}), [3] a 140 g/m^2 polypropylene thermally-bonded nonwoven geotextile (GT_{tb-nw}), and, [4] a geogrid/geotextile composite using a welded polypropylene biaxial geogrid with a 151 g/m^2 polypropylene needlepunched nonwoven geotextile firmly bonded between the cross laid reinforcement ribs ($GC_{gg-nwgt}$). The relevant properties of these four materials are shown in Table 1.

Table 1. Geosynthetic Characteristics Based on Manufacturer's Literature

Geosynthetic	Property		
	T_{ult} MD/XD (kN/m)	$T_{2\%}$ MD/XD kN/m)	$T_{junction}$† MD/XD (kN/m)
GG_{wd-pp}	30 / 30	10 / 10	9.0 / 9.0
GT_{np-nw}	6.0 / 10.0	NA‡	NA‡
GT_{tb-nw}	na	NA‡	NA‡
$GC_{gg-nwgt}$	30 / 30	13 / 13	NA‡

na Not available
†Junction Strength measured using Geosynthetic Research Institute GRI-GG2 Method B
‡Not Applicable

2.2 Subgrade and Aggregate Base Material

Micaceous sandy silt (ML-MH) from Georgia was used for the subgrade. This residual soil was selected based on its problematic construction characteristics that include pumping and weaving at near optimum moisture contents, which usually requires chemical or mechanical stabilization, especially when wet of optimum (as is most often the case). These soils are also characterized by a relatively fast dissipation of pore water pressure as opposed to more cohesive soils, which is also a consideration for their selection. The soil was provided by Georgia Department of Transportation. Gradation tests (ASTM D422 and D1140) indicated 95% passing 1 mm and 65% passing 0.075 mm. The soil was found to have a maximum dry unit weight of about 17.1 kN/m^3 at an optimum moisture content of 17% based on standard Proctor moisture density tests (ASTM D698); however, the soil has a natural moisture content of over 40% as delivered to the laboratory.

The base course material used in all test sections was a graded aggregate base material meeting Georgia Department of Transportation specifications. Standard Proctor compaction test (ASTM D698) and gradation tests were performed on the aggregate base course. The aggregate has a maximum dry unit weight of 22.8 kN/m^3 at an optimum moisture content of 5.4%. The gradation results indicated that the aggregate is a well-graded gravel with 100% smaller than 20 mm and 8% finer than 0.075 mm. The graded aggregate base is estimated to have a friction angle of 43° based on large direct shear tests that had been previously performed on similar materials by the laboratory performing the stabilization tests.

2.3 Test Section Construction

The silt type subgrade material was placed at a moisture content of approximately 31% to produce a CBR value of approximately 1% (the common saturated CBR value for this material in the field) under the applied compaction effort. The subgrade was constructed in 150 mm lifts and compacted with a gasoline powered "jumping jack" trench compactor.

The CBR was controlled during placement of each lift in the test sections using measurements of both moisture content and vane shear strength. Laboratory tests indicated that a vane shear strength of 30 kPa correlated directly to a CBR=1 for the silt type soil. Periodically, bulk density measurements were also taken with a nuclear densometer. Vane

shear tests were performed subsequent to final compaction and leveling of the subgrade, and immediately prior to placement of the aggregate base.

The final subgrade surface was surveyed and the reinforcement was placed directly on top of the subgrade layer. One edge of the geosynthetic reinforcement was extended through a slot in the test box face in order to monitor movement of the geosynthetic at the edge of the box during testing.

The base course material was placed at a target water content of approximately 6% and in two 150-mm thick lifts for a total thickness of 300 mm. Compaction was achieved with an 8-hp vibratory plate compactor. Density measurements taken with a nuclear densometer indicated an average dry density of 20.8 kN/m^3 with a coefficient of variation of 3%.

The aggregate layer thickness was designed to result in 76 to 100 mm of rutting under moderate traffic (1000 cycles) based on the procedures outlined in the FHWA Geosynthetics Design and Construction Guidelines (Holtz et al., 1998). The FHWA charts indicate that a 300 mm base course layer is required to limit the rut depth to 76-100 mm for moderate traffic ($\approx$ 1000 cycles) of an 80 kN axle load for a CBR=1 subgrade.

3 STABILIZATION TEST RESULTS

The primary results of the stabilization tests are in terms of the deformation response of the aggregate layer. The number of cycles was adjusted to provide an equivalent performance under a uniform 500 kPa applied stress condition using an equivalent load factor from a 4th order polynomial equation, similar to that used for traffic simulation, with the load factor calculated as:

$$\text{Load Factor} = (\text{Actual Load / Target Load})^4$$

The load factor was applied to each recorded cycle with the cumulative load cycles used in the plots. This does not affect the magnitude of deformation or the shape of the curve, but shifts the curve by reducing the number of cycles for a given deformation to account for load reductions that occurred during several of the tests.

Figure 2 provides a summary of the permanent deformation response for a wheel pressure normalized at 500 kPa for test sections constructed with 300 mm of aggregate and a subgrade CBR=1. Table 2 provides a comparison of the performance characteristics from each test section, including the

number of cycles and the corresponding Traffic Benefit Ratio (TBR) for each of the test results at 25 mm and 76 mm of rutting. Also shown is the maximum strain measured in the geosynthetic and the rut bowl dimensions at the end of the tests. Table 2 also presents the corresponding deformation response measured on the geogrid. Finally, Figure 3 shows the pore pressure response measured in the subgrade during cyclic loading.
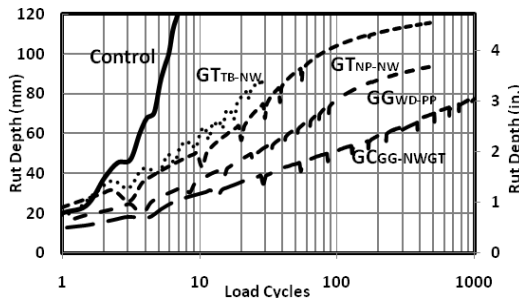

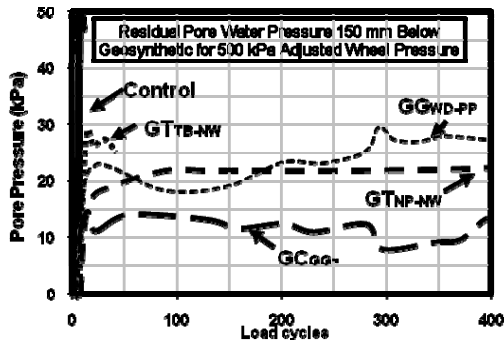Figure 2. Permanent deformation response versus load cycles for the CBR=1 subgrade.

Figure 3. Pore pressure in subgrade versus load cycles for CBR=1 subgrade.

Table 2. Performance Characteristics of Each Test Section

	Test Section				
	Control	GG_{wd-pp}	GT_{np-nw}	GT_{tb-nw}	$GC_{gg-nwgt}$
Number of Cycles					
25-mm rut	1.5	4.5	1.2	1.5	6.5
76-mm rut	5	97	31	19	855
TBR					
25-mm rut	1	3	0.8	1	4.3
76-mm rut	1	19.4	6.2	3.8	171
Maximum Measured Strain in Geosynthetic					
Residual strain		2.8	1.6	2.0	3.8
Average outside platen		0.93	1.8	0.95	0.70
Edge of rut bowl		2.5	2.7	2.7	2.0
Subgrade Permanent Deformation Bowl at End of Test					
Diameter (mm)	710	798	798	798	798
Depth (mm)	115	69	89	64	79

The test sections were excavated after the cyclic test was completed to develop profiles of the subgrade permanent deformation bowl (i.e., rut bowl profile) and to evaluate the integrity of the geosynthetics. During the excavation, observations of the base, the imprint of the geogrid remaining on the geotextile, and imprint of the geogrid on the subgrade were observed for indications of separation performance and the level of slippage. The measured subgrade rut bowl depth and diameter are provided in Table 2.

4 DISCUSSION OF RESULTS

The results from Figure 2 and Table 2 clearly show a difference in the performance of the geosynthetics evaluated in this study with $GC_{gg-nwgt}$, the geogrid/nonwoven geocomposite, performing the best of all materials tested. The geocomposite test reached over 850 cycles of loading before 76 mm of rutting occurred and had a TBR value of over 170.

The open geogrid GG_{wd-pp} placed directly on the subgrade may be at a disadvantage with this type of soil. The soil can easily be penetrated by gravel particles and thus some of the deformation may be the result of aggregate penetration until interlock is developed. Also, the gradation of the soils indicates that the ability of the gravel does not meet standard filter/separator criteria for the silt (e.g., the D15 of the gravel {i.e., 0.3 mm} is greater than 5 times the D15 of the subgrade {i.e., 0.005 mm}; Bertram, 1940). Regardless, the geogrid provided significant improvements in deformation response over the control with a TBR value of 19 as shown in Table 2.

The GG_{wd-pp} placed over the GT_{np-nw} (needlepunched nonwoven geotextile) or the over the GT_{tb-nw} (thermally-bonded nonwoven geotextile) did not perform as well as the $GC_{gg-nwgt}$. The higher deformation response is attributed to sliding of the geogrid over the nonwoven geotextiles, which was apparent due to movement at the front of the box during the test and from the imprint of the geogrid on the geotextile observed during excavation. Sliding is also indicated by comparison of the strain in the GG_{wd-pp} geogrid placed over both geotextiles compared to the strain in the $GC_{gg-nwgt}$ geogrid/geotextile composite material. A distinct reduction in strain occurred between 70 and 100 cycles of loading, which would result from a reduction in interaction associated with sliding.

GG_{wd-pp} over the GT_{np-nw} performed better than GG_{wd-pp} over GT_{tb-nw}. Visual measurements at the front of the box indicated greater movement and sliding occurred at the interface of the geogrid and

the slicker thermally-bonded nonwoven geotextile compared to the needlepunched nonwoven geotextile. In addition, the lower permeability of the thermally-bonded nonwoven likely contributed to the poorer performance as discussed below.

A summary of the pore pressure response for the test sections is shown in Figure 3. The pore pressure corresponds somewhat to the results of Figure 2 with high initial pore pressure developing for the test section where the largest amount of deformation per cycle was measured (i.e., GG_{wd-pp} geogrid placed over the GT_{tb-nw}) and the lowest pore pressure developing for the section with the least amount of deformation per cycle (i.e., $GC_{gg-nwgt}$). As indicated in the previous paragraph, sliding contributed to the poorer performance of the GG_{wd-pp} placed over the GT_{tb-nw}. The lower permeability of the thermally-bonded nonwoven versus the needlepunched nonwoven may have also contributed to the higher pore water pressure measured in that test section. The pore water pressure results indicate that disturbance due to aggregate penetration into the subgrade in the control section and the GG_{wd-pp} open geogrid section also leads to high pore water pressure.

The increase in pore water pressure reduces the effective strength of the soil, resulting in an undrained subgrade strength that is actually less than CBR=1 and correspondingly increased rutting occurs (see Christopher et al., 2009). This rapid pore pressure build up does not occur in the geocomposite due to the separation, i.e. prevention of the point stress that occurs during aggregate penetration and in-plane drainage allowing for more rapid pore pressure dissipation.

5 CONCLUSIONS

The results of full-scale laboratory tests on geogrid, geogrid placed over geotextile, and geocomposite reinforced unpaved roadway section are comparatively presented. A control section containing no reinforcement showed a rapid increase in rutting with applied cyclic pavement load, reaching 76 mm of rut depth in 5 load cycles. Measurements of pore water pressure in the subgrade indicate a correspondingly rapid increase in pore water pressure, reaching a value of 58 kPa. A test section with an open geogrid showed a marked improvement in rutting behavior such that 97 load cycles were applied before reaching 76 mm of rut and the maximum pore water pressure was measured at 29 kPa. The section with the geocomposite showed the best performance both in terms of rutting

and pore water pressure development. In this section, 855 load cycles were applied before a rut depth of 76 mm was seen and the peak pore water pressure quickly reached a maximum value of 16 kPa. The section with geogrid placed over a nonwoven geotextile, namely the GT_{np-nw}, underwent 31 cycles of loading to reach a rut depth of 76 mm and the maximum pore water pressure was 23 kPa during the test. For geogrid placed over a thermally-bonded nonwoven geotextile, the GT_{tb-nw}, 19 cycles of applied load and maximum pore water pressure of 30 kPa were reached during testing.

These results indicate that the manufactured geocomposite material showed better performance in rutting and pore water pressure development than placement of the geogrid over the nonwoven geotextiles tested and also the geogrid used alone. The geogrid provided interlocking effects with the aggregate base and the geotextile provided separation and filtration effects at the subgrade/aggregate interface. When the geogrid overlied the geotextiles, slippage along the interface of the materials was observed and effectively less improvement in performance was found compared to the bonded geocomposite. Additional tests are ongoing with other types of geogrid and geotextile combinations to support this initial work and will be reported in a future paper.

REFERENCES

AASHTO (2001). G*eosynthetic Reinforcement of the Aggregate Base Course of Flexible Pavement Structures – PP 46-01*, Standard Specifications for Transportation Materials and Methods of Sampling and Testing, 26th Edition, and Provisional Standards, American Association of State Transportation and Highway Officials, Washington, D.C.

AASHTO, 1993. *AASHTO Guide for Design of Pavement Structures,* American Association of State Highway and Transportation Officials, Washington, D.C.

ASTM, 2006. *Geosynthetics*, Annual Books of ASTM Standards, Vol. 4.13, American International, West Conshohocken, PA.

ASTM, 2007. *Soil and Rock*, Annual Books of ASTM Standards, Vol. 4.08 and 4.09, American International, West Conshohocken, PA.

Berg, R.R., Christopher, B.R., and Perkins, S.W. 2000. *Geosynthetic Reinforcement of the aggregate Base/Subbase Courses of Pavement Structures*, prepared for AASHTO Committee 4E by the Geosynthetic Materials Association, 176 p.

Bertram, G.E. 1940. *An Experimental Investigation of Protective Filters*, Publications of the Graduate School of Engineering, Harvard University, No. 267, January, 1940.

Christopher, B.R. and Lacina, B. 2008. "Roadway Subgrade Stabilization Study", Proceedings of GeoAmericas 2008, Cancun, Mexico, 2008, International Geosynthetic Society, pp. 1013–1021.

Christopher, B.R. and Perkins, S.W. 2008. "Full Scale Testing of Geogrids to Evaluate Junction Strength Requirements for Reinforced Roadway Base Design," Proceedings of the Fourth European Geosynthetics Conference, Edinburgh, United Kingdom, International Geosynthetics Society.

Christopher, B.R.. Perkins, S.W., Lacina, B. and Marr, W.A. 2009. "Pore Water Pressure Influence on Geosynthetic Stabilized Subgrade Performance," Proceedings of Geosynthetics 2009, Salt Lake City, USA, Industrial Fabrics Association International, pp. 215-221.

Holtz, R.D., Christopher, B.R., and Berg, R.R. 1998. *Geosynthetic Design and Construction Guidelines*, U.S. Department of Transportation, Federal Highway Administration, Washington DC, Report No. HI-95-038, 1995 (revised 1998 and 2998), 396 p.

Jornby, B.N. and Hicks, R.G. 1986. *Base Coarse Contamination Limits*, Transportation Research Record, No. 1095, Washington, D.C.

Perkins, S.W. 1999. *Geosynthetic Reinforcement of Flexible Pavements: Laboratory Based Pavement Test Sections*, Montana Department of Transportation, Helena, Montana, Report No. FHWA/MT-99/8106-1, 140 p.

Perkins, S.W. 2002. *Evaluation of Geosynthetic Reinforced Flexible Pavement Systems Using Two Pavement Test Facilities*, U.S. Department of Transportation, Federal Highway Administration, Washington, DC, Report No. FHWA/MT-02-008/20040, 120 p.